IMPLEMENTATION OF CSAR IMAGING ALGORITHM USING WAVEFRONT RECONSTRUCTION THEORY

M.Poornima Pranayini, Naveen Namdeo, P.Dhanalakshmi

ABSTRACT: Circular synthetic aperture radar is a SAR mode where the radar-carrying platform moves in a circular path. This paper deals with the design, simulation and implementation of a new algorithm for squint mode operation Circular Synthetic Aperture Radar applicable for curved trajectory of the platform. This is a squint CSAR imaging algorithm where, first the raw-data is transformed to the polar spatial frequency domain using along-track varying kernels and then converted to rectilinear samples. The proposed algorithm will be validated by developing a simulation model in MATLAB and verifying the results with known set of test data.

I.INTRODUCTION:

Synthetic Aperture Radar (SAR), with its ability to provide high-resolution and large-area imaging has been an important tool for civilian and military applications. Similar to any other radar imaging modalities, SAR techniques collect the reflections from an irradiated area and process them to create a reflectivity map from the scattering bodies present in the imaged region. The SAR data acquisition process can be described as follows.. Along the scanned trajectory, an illuminating source radiates a waveform and records the collected reflections from the objects inside the scan area.

The recorded reflections are processed to eliminate the distortions caused by the antenna, the shape of the irradiated waveform, and the motion of the moving platform. Finally, the resulting reflectivity map can be visualized and interpreted. Most conventional SAR systems operate along a straight path at a certain altitude with respect to the ground plane. Such linear SARs are associated with the problem that a target SAR signature with sufficiently high signal-to-noise power ratio can be measured only over a limited aspect angle interval. This is due to the fact that a target can present different signatures depending on its orientation with respect to the scan geometry.

The amount of power reflected from a given target varies according to the dielectric contrast between the target and the propagation medium, the relative reflecting area of the target when viewed from the illuminating location, and the radiated power density. The signature variations may complicate the interpretation of the target locations and orientations in the resulting SAR images. A new imaging mode, the Circular Synthetic Aperture Radar, can be used to circumvent this problem.

In a Circular Synthetic Aperture Radar System, the radar-carrying platform at a fixed point moves along a circular path while the radar beam illuminates the ground region that falls inside the scanning circle. A circular aperture can be realized by either using an array of sensors or by moving one sensor on a circular trajectory generating a synthetic aperture of circular shape [5]. A CSAR thus provides an all-directional observation, high spatial resolution and 3-Dimensional imaging.

One of the distinguishing features of Circular Synthetic Aperture Radar is that the raw-data is collected in polar format. This makes all the existing image formation algorithms unsuitable for CSAR as conversion to spatial domain cannot be directly performed using FFT.

Several reconstruction approaches have been proposed for this SAR modality, including Time Domain Correlation (TDC) techniques and Plane Wave Approximation (PWA) methods. However, TDC techniques have execution times in the order of days or even weeks and PWA methods produce images with low focal quality, considerable spatial location errors and target smearing [10, 11]. An alternative approach is the use of waveform reconstruction techniques. These methods are based on performing a series of operations in the frequency domain that transfer the collected data from the spatiotemporal domain in which it was originally collected to the spatial domain where it will be displayed. It has been shown that wavefront reconstruction techniques produce spatially accurate CSAR images0.

ISSN: 2278 – 7798

II.PROPOSED METHOD:

A. System model:

This paper provides a wavefront-reconstruction theory based imaging method for circular synthetic aperture radar imaging from the slant plane CSAR data collected over a partial segment of a circular flight path. This technique uses the multidimensional impulse response or the slant plane green's function of the imaging system. The signal model considered is as in figure 1.

The radar-carrying aircraft moves along a circular path with radius R_g on the plane $z=Z_c$ with respect to the ground plane. As the radar moves along the circular synthetic aperture, its beam is spotlighted on the disk of radius R_0 (w) centered at the origin of spatial domain on the ground plane.

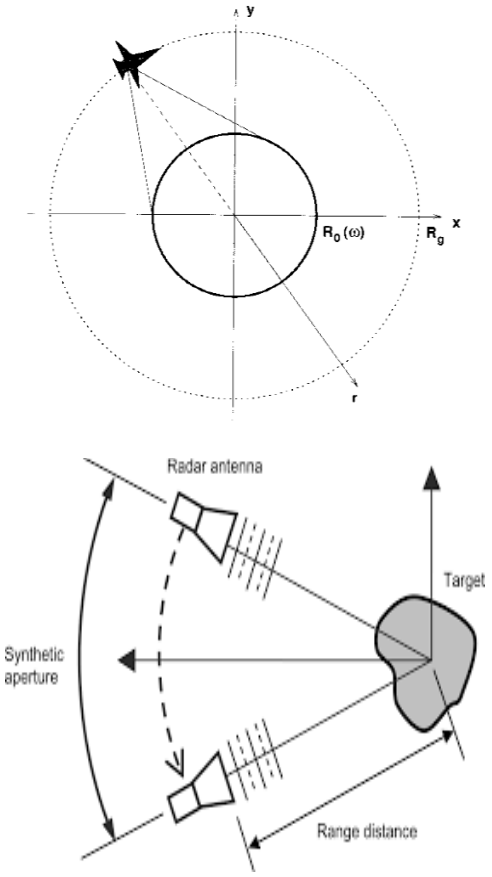

Figure.1

The measured CSAR signal in the fast time and slow-time domains (t ,θ) is defined by:

$$s(t,\theta) = \iint f(x,y)p[t - \frac{2\sqrt{(x-Rg\cos\theta)^2+(y-Rg\sin\theta)^2+Zc^2}}{c}]dxdy$$

-equation 1

The Fourier Transform of the model with respect to fast time, t, is

$$s(\omega,\theta) = P(\omega)\iint f(x,y)conj\big(g\theta(\omega,x,y)\big)dxdy$$

-equation 2

Where g_θ is the CSAR imaging system shift-varying impulse response (slant plane Green's function) at the slow time θ and fast-time frequency w.

This data is called the slant plane CSAR data which in our algorithm is converted to ground plane data s_g which is used for the reconstruction algorithm. The slant plane to ground plane conversion is done using the shift varying impulse response linear system kernels.

B. Slant Plane Green's Function:

The slant plane Green's function in the polar spatial frequency domain is defined as:

$$G\theta p(\omega,\rho,\varphi) = W1(\theta-\varphi)W2(\omega,\rho) \times e^{(-j\sqrt{4k^2-\rho^2}Zc - j\rho Rg\ \cos\theta-\varphi)}$$

Where, $W_1(\varphi)=1$ for $|\varphi| \le \theta x(\omega)$

=0 otherwise

$W_2(w,\rho)=1$ for $|\rho - 2k\cos\theta z| \le 2k\,(\sin\theta z)^2 \sin\theta x\,(\omega)$

=0 otherwise

For the ground plane scenario, that is, $\theta_z=0$, the Green's function spectrum is a pole distribution on the circle of radius 2k. It possesses a very low energy spread around this circle which corresponds to evanescent waves (the waves from targets where the range is significantly greater than the radar and which cannot be recorded by a realistic radar).

For the slant plane problem, that is, $\theta_z \neq 0$, the Green's function possesses a spatial frequency spread around the circle of radius $\rho=2k\cos\theta_z$ in the spatial domain which increases as the $R_0(w)$ increases. This is because a non-zero slant makes the radar signal experienced by the

ISSN: 2278 – 7798

ground targets to have a wavelength other than $2\pi c/w$ which varies with (x,y,θ).

C. **Reconstruction**:

The proposed CSAR imaging utilizes a two-step reconstruction algorithm-The first is the conversion of slant plane to ground kernel using the system kernel and the second stage is the Ground plane CSAR reconstruction. The CSAR signal of equation 2 can be modified using the parseval's theorem and then making variable transformations from rectilinear spatial frequency (k_x,k_y) domain to the polar spatial frequency (φ,θ) domain as

$$s(\omega,\theta) = P(\omega)\iint \rho Fp(\rho,\varphi)conj(G\theta p(\omega,\rho,\varphi)d\rho d\varphi$$

-equation 3

Where the analytical slant plane Green's function $G_{\theta p}$ is given by:;

$$G_{\theta p}=e^{j\sqrt{4k^2-\rho^2}Zc+j\rho Rg\ \cos(\theta-\varphi)}$$

a. Slant plane to ground plane conversion:

The first phase of developing CSAR reconstruction is the conversion of slant plane data to a database of the target region which is collected at the ground plane, that is, at zero altitude. The CSAR model from equation 3 can be re-written as:

$$s(w,\theta) = \int \Lambda(\omega,\omega g)sg(\omega g,\theta)d\omega g$$

Where,

$$\Lambda\ (w, w_g) = P(\omega)W2(\omega,\rho)e^{-j\sqrt{4k^2-\rho^2}Zc}$$

-equation 4

And

$$s_g(w_g,\theta)=\rho\int F_p(\rho,\varphi)W1(\theta-\varphi)e^{-j\rho R_g\cos(\theta-\varphi)}d\varphi$$

Where $s_g(w_g,\theta)$ is called the ground plane CSAR signal which is nothing s at z=0 with a radar whose fast-time frequencies are labeled by w_g.

The slant plane system model and ground plane system model can be related using a linear system kernel whose input is the ground plane signal $s_g(w_g\theta)$ and the shift-varying impulse response is $\Lambda(w,w_g)$ and generates the output slant plane CSAR signal $s(w,\theta)$. This kernel for conversion of ground plane to slant plane is known as analytical signal.

The inverse of the analytical system takes slant plane signal as input and generates the ground plane signal, and its impulse response is denoted by $\Lambda^{-1}(w_g,w)$.

The inverse system kernel can be the pseudo-inverse of the analytical kernel. In this algorithm, since we have the slant plane signal as the raw data, we first construct the inverse system kernel. This was found by constructing the analytical function and then taking its pseudo-inverse. With the two inputs then we calculate the ground plane signal which is further used in the reconstruction.

b. Ground plane CSAR reconstruction:

The second stage, that is the actual reconstruction part has been performed based on the wavefront reconstruction theory. In order to properly visualize the recorded reflections, the effect of the scan geometry must be compensated and the data must the migrated from the polar space to the rectangular space where it will be visualized and interpreted. This has been accomplished stage by stage using the below described algorithm.

Calculate the fast time matched filtering of the slant plane CSAR signal with filter response centered at a reference point $T_c=2R_c/c$.

$$s(t,\theta) = s(t,\theta) * p_0^*(-t)$$

For generating the ground plane reference signal for reconstruction we first obtained the slant plane signal, $s(w,\theta)$ by taking the one-dimensional Fourier transform of the above matched filtered output with respect to fast time t. This signal is modified using equation 4 to move the fast-time origin back to actual fast-time zero, t=0 from the point $t=t-T_c$.

$$s(\omega,\theta) = s(\omega,\theta)e^{(-j\omega\,T_c)}$$

-equation 5

This signal is then multiplied with the inverse system kernel $\Lambda^{-1}(\omega_g,\omega)$ obtained by calculating the pseudo-inverse of the analytical system $\Lambda(\omega,\omega_g)$ to give the ground plane CSAR data $s_g(\omega_g,\theta)$ at a fixed radar look angle, θ as:

$$s_g(\omega_g,\theta) = \int \Lambda^{-1}(\omega_g,\omega)s(\omega,\theta)d\omega$$

For a partial rotation aspect angle measurement, zero-pad the $s_g(\omega_g,\theta)$ in the slow-time domain θ to avoid the circular convolution aliasing experienced by the slow-time frequency filter due to the smaller aspect angle interval, by

ISSN: 2278 – 7798

$$\pm \frac{R_0(\omega_{min})}{R_g}$$

Now the zero-padded ground plane data is subject to discreet Fourier transform with respect to the available slow-time domain, θ, samples which yields the two-dimensional ground plane spectrum $S_g(\omega, \xi)$. The target function in the (ρ,ξ) domain is constructed by performing the slow-time frequency domain matched filtering, with $\rho = 2\omega_g / c$ as

$$F_p(\rho, \xi) = S_g(\omega_g, \xi) S_{g0}^*(\omega_g, \xi)$$

The polar samples of the target function in the spatial frequency domain $F_p(\rho, \theta)$ were then obtained by performing inverse discreet Fourier transform of the target function $F_p(\rho, \xi)$ with respect to ξ.

This target function polar data spectrum has been converted to rectilinear spectrum $F(k_x, k_y)$ via a two-dimensional interpolation. This gives evenly-spaced samples of the target function spectrum $F(k_x, k_y)$. The conversion is based on the equations:

$$k_x = \rho \cos\theta$$

$$k_y = \rho \sin\theta$$

-Equation 6

The last stage of reconstruction is the reconstruction of the actual target function. Two-dimensional inverse DFT of the target spectrum was calculated to reconstruct the samples of the target function f(x,y) in the spatial domain.

III. RESULTS:

The proposed algorithm is tested with a five-point target for a partial rotation of the radar-carrying aircraft over an arc length of 200 meters.

The radar is pulsed radar where the pulse width is 38μs and the carrier frequency is 9.4GHz. The measured target signal generally called the raw data which has been generated using equation 1 is observed as in Figure.2. This raw-data is for five point target.

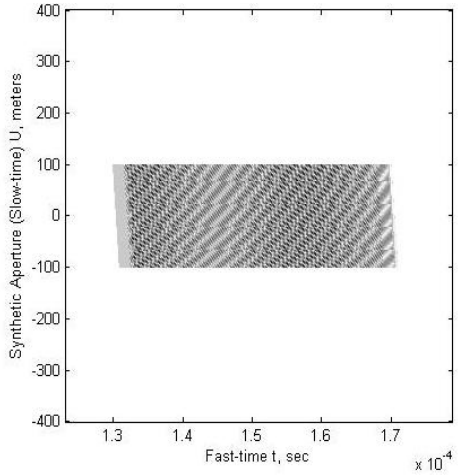

Figure.2: Measured CSAR signal

This raw data is then used for reconstruction after certain transformations as per the algorithm.

The next stage is the time domain or range compression of the Fourier transform of the raw data signal measured. The compression is performed by correlating each of received pulse is with a matched filter which is delayed version of transmitted pulse. The compressed signal spectrum is observed as in figure 3.

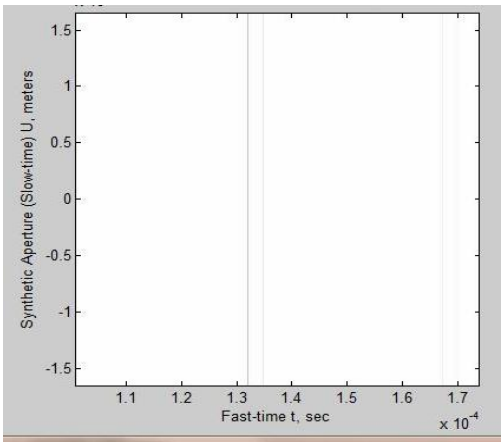

Figure 3: Range compressed signal spectrum.

After this stage the slant plane to ground plane conversion is performed for which azimuth compression or slow-time matched filtering is performed. The slow-time matched filtering is performed by correlating the data across all pulse returns from a given range with a matched filter.

This signal was then interpolated to convert the unevenly spaced spatial frequency domain polar samples of the CSAR signal to evenly spaced spatial frequency domain rectilinear samples which can then be used for reconstruction. The conversion has been performed using the equation 6.

ISSN: 2278 – 7798

The reconstructed spectrum has been observed as in figure.4

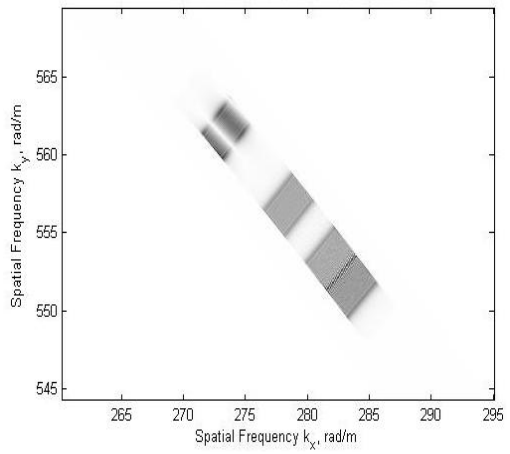

Figure.4: Wavefront CSAR reconstruction spectrum

The reconstructed signal shows the five point-targets as five dots positioned at their respective co-ordinates. This signal is only in two-dimensions as the signal considered is the ground plane signal where the third dimension, i.e., elevation is made null.

The five-point target reconstructed CSAR signal has been observed as in Figure.5.

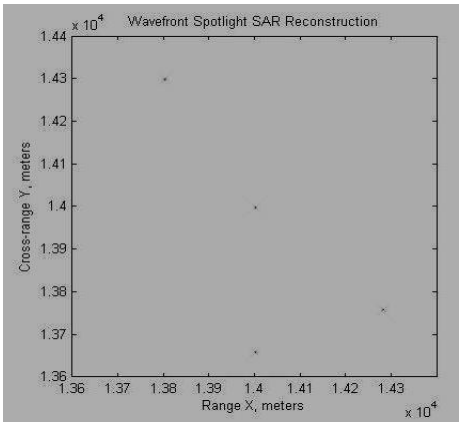

FIGURE.5: Wavefront reconstructed CSAR signal

IV. REFERENCES:

[1] http://www.jpier.org/PIERB/pierb02/03.07110101.pdf.

[2] http://www.sea-mist.se/tek/rcg.nsf/attachments/LicThomas_pdf/$file/LicThomas.pdf

[3] http://ieeexplore.ieee.org/xpl/login.jsp?tp=&arnumber=6581140&url=http%3A%2F%2Fieeexplore.ieee.org%2Fxpls%2Fabs_all.jsp%3Farnumber%3D6581140

[4] http://www.jpier.org/PIER/pier.php?paper=11082201

[5] http://www.adv-radio-sci.net/4/85/2006/ars-4-85-2006.pdf

[6] http://asp.eurasipjournals.com/content/2010/1/657323

[7] http://ieeexplore.ieee.org/xpl/articleDetails.jsp?arnumber=6750510

[8] M. Soumekh, Synthetic Aperture Radar Signal Processing with MATLAB Algorithms, Wiley-Interscience, New York, NY, USA, 1999.

[9] https://engineering.purdue.edu/~bethel/sar_image_formation.pdf

[10] J. Curlander and R. McDonough, Synthetic Aperture Radar: Systems and Signal Processing, Wiley-Interscience, New York, NY, USA, 1991.

[11] A. Ausherman, A. Kozma, J. L. Walker, H. M. Jones, and E. C. Poggio, "Developments in radar imaging," IEEE Transactions on Aerospace and Electronic Systems, vol. 20, no. 4, pp. 363–400, 1984.

[12] Soumekh, "Reconnaissance with slant plane circular SAR imaging," IEEE Transactions on Image Processing, vol. 5, no. 8, pp. 1252–1265, 1996.

[13] J. Burki and C. F. Barnes, "Slant plane CSAR processing using householder transform," IEEE Transactions on Image Processing, vol. 17, no. 10, pp. 1900–1907, 2008.

[14] https://www.sbir.gov/sbirsearch/detail/309006

[15] https://www.safaribooksonline.com/library/view/synthetic-aperture-radar/9780471297062/Chapter07.html

[16] http://num.math.uni-goettingen.de/~r.luke/publications/LukeBurkeLyonsSIREV02.pdf

[17] http://proceedings.spiedigitallibrary.org/proceeding.aspx?articleid=906518

[18] Mehrdad Soumekh. **Wavefront-Based Synthetic Aperture Radar Signal Processing**. *EUSAR 2000 Special Issue, Frequenz, Zeitschrift für Telekommunikation (Journal of Telecommuni cations)*, 55:99-113, March/April 2001.

[19] http://www.dtic.mil/dtic/tr/fulltext/u2/a443066.pdf

[20] A. Papoulis, Systems and Transforms with Applications in Optics, McGraw-Hill, New York, NY, USA, 1968.

[21] D. Flores-Tapia, G. Thomas, and S. Pistorius, "A wavefront reconstruction method for 3-D cylindrical subsurface radar imaging," *IEEE Transactions on Image Processing*, vol. 17, no.10, pp. 1908–1925, 2008.

[22] M. Soumekh, "Band-limited interpolation from unevenly sampled data," IEEE Transactions on Acoustics, Speech, and Signal Processing, vol. 36, no. 1, pp. 110–122, 1988.

[23] G. Franceschetti, Synthetic Aperture Radar Processing, CRC Press, Boca Raton, Fla, USA, 1999.

[24] B. Edde, Radar: Principles, Technology and Applications, Prentice-Hall, Upper Saddle River, NJ, USA, 1995

ISSN: 2278 – 7798